UDC 544.72
https://doi.org/10.15407/kataliz2023.34.073

The influence of mechanochemical and microwave modification on the properties of SnO_2 as photocatalyst

Mariia M. Samsonenko, Svitlana V. Khalameida

Institute for Sorption and Problems of Endoecology of National Academy of Sciences of Ukraine
13 Naumov Str., Kyiv, 03164, Ukraine, e-mail: mashuna.08@gmail.com

Samples of precipitated SnO_2 were modified by means of mechanochemical and microwave treatment. Physicochemical properties of all samples were investigated using DTA, XRD, FTIR spectroscopy, nitrogen adsorption-desorption and UV-Vis spectroscopy. Photocatalytic activity was evaluated using the degradation of rhodamine B and safranin T under Vis-irradiation. It was found that the initial precipitated and modified samples correspond to the composition of tin oxyhydroxide - SnO(OH)x. It has been established that as a result of mechanochemical and microwave treatment of tin oxyhydroxide in the wet gel stage, it is possible to obtain photocatalytically active materials with a uniform mesoporous structure and high specific surface area and a band gap of about 3.5-3.6 eV. A peculiarity of the mechanochemical treatment of xerogels in water is the formation of a meso-macroporous structure. Relationship between physicochemical and photocatalytic properties of prepared samples has been discussed. The dependence of the efficiency of photocatalytic degradation of dyes on changes in the porous structure, the presence of defects on the surface of the catalyst, and its electronic characteristics was established.

***Keywords**:* SnO_2, mechanochemical and microwave treatment, porous structure, photocatalytic activity, dyes, Vis-irradiation

Introduction

Tin dioxide is one of the wide-gap semiconductor materials with a complex of physicochemical and functional properties [1-3]. Its characteristics determine the possibility of using SnO_2 in adsorption and catalytic processes aimed at monitoring the condition and protecting the environment. For example, extraction of ions from wastewater and natural waters, photocatalytic degradation of pollutants in the aquatic environment and determination of the content of harmful substances in the air, etc. [1-5].

The efficiency of SnO_2 in these processes is determined by a set of physical and chemical properties, namely its crystalline and porous structure, specific surface area, morphology, surface condition, thermal and mechanical stability, and the possibility of granulation. The complex of specified characteristics should have optimal values for the effective use of tin dioxide in adsorption and catalytic processes.

Regulation of the physicochemical characteristics and, as a result, the functional properties of precipitated tin dioxide can be carried out both at the synthesis stage (traditional deposition, sol-gel method and template synthesis), and through its following treatment – "post-synthetic modification" [6] (thermal and hydrothermal treatment). It is known that SnO_2 precipitated from aqueous solutions is, as a rule, an amorphous hydrated oxide with a high specific surface area and a microporous structure, with a band gap in the range of 4.2-3.6 eV. The use of various methods of synthesizing tin dioxide from aqueous solutions allows to vary the physicochemical parameters of the obtained samples only to a certain extent. In particular, it is difficult to obtain a developed mesoporous structure using the sol-gel method and deposition, but it is possible when using the template method. Also, only the template method of synthesis allows forming the perfect crystalline structure of cassiterite. In addition, these methods of synthesis have a number of difficulties and disadvantages in their practical application: the use

of a significant amount of water for washing samples makes them eco-insensitive, and the use of expensive templates and precursors, the need for high temperatures for annealing the templates - expensive and energy-consuming. In turn, thermal and hydrothermal treatments are widely used as methods of modifying oxide materials, in particular for tin dioxide. These types of processing make it possible to widely vary the physicochemical parameters of tin dioxide samples processed in the form of gels and xerogels, in particular textural characteristics [7]. But the use of thermal treatment doesn`t allow reducing the absorption edge and the width of the band gap of tin dioxide to the dimensions that condition activity in visible light. At the same time, hydrothermal treatment requires fairly harsh conditions and the use of special equipment that operates at high temperatures and pressures. Therefore, there is a need to develop cheaper, environmentally friendly and simple methods of synthesis and modification.

There is a group of simpler and more effective methods of "green chemistry" for the synthesis and modification of catalysts and sorbents, which use non-convective energy supply to the system [8-11]. They allow to obtain results close to those for hydrothermal method, but using simpler equipment and lower temperatures, as well as significantly reduce the duration of the process. In addition, despite a significant number of publications, research in these areas continues to actively develops. Thus, recently, the rapid development of mechanochemistry and its prospects for the chemical synthesis and modification of oxide materials, as well as the conduct of catalytic reactions under MChT, was recently recognized at the level of the International Union of Theoretical and Applied Chemistry (IUPAC) [12]. Despite the large number of publications devoted to mechanochemical treatment (MChT) of oxide materials, their number is insignificant for tin dioxide. The existing works describe only the mechanochemical synthesis of tin (II) oxide followed by its transformation into tin (IV) oxide during thermal treatment at 350-800 °C. In turn, microwave treatment (MWT) is a promising method that allows to realize hydrothermal conditions in a more economical and ecologically beneficial way and to vary the parameters of the crystalline and porous structure of tin dioxide. However, post-synthetic modification of SnO_2 powders and xerogels and the study of the effect of these treatment methods on the surface structure and parameters of the crystalline, porous, and electronic structures, as well as the functional properties of tin dioxide, remain almost unexplored. Thus, the advantages and efficiency of using these methods to modify other oxides and hydroxides make them interesting and relevant for the search for ways to modify laboratory and commercial samples of tin dioxide.

Experiment

Synthesis of SnO_2 samples. Two series of tin dioxide samples were obtained by heterogeneous and homogeneous precipitation from water solutions (Fig. 1).

Modification of SnO_2 samples. Wet gels and xerogels were subjected to mechanochemical and microwave treatments. Mechanochemical treatment was carried out using a planetary ball mill "Pulverisette-7" ("Fritsch", Germany) in air and water for 0.5 h at 300 and 500 rpm. High-pressure reactor "NANO 2000" ("Plazmotronika", Poland) was used for microwave treatment. It was carried out at temperatures of 165-235 °C for 0.5-1 hours.

Physicochemical studies of modified samples. The physicochemical properties of the modified samples were investigated by the following methods. Differential thermal analysis (DTA-TG) was carried out using the Derivatograph-C device in the temperature range of 20-800 °C and heating rate of 10°C/min. XRD analysis was performed on a Philips PW1830 diffractometer with CuKα radiation (λ = 0.15406 nm). The crystallite sizes L were calculated using the Debye-Scherrer equation (1):

$$L = \frac{0.89 * \lambda}{\beta * \cos\theta}, \quad (1)$$

where 0.89 is a constant, λ = 0.154 nm is the wavelength, nm, β is the width at half height of the peaks, measured from the diffractogram, degrees, Θ is the Bragg angle from the diffractogram.

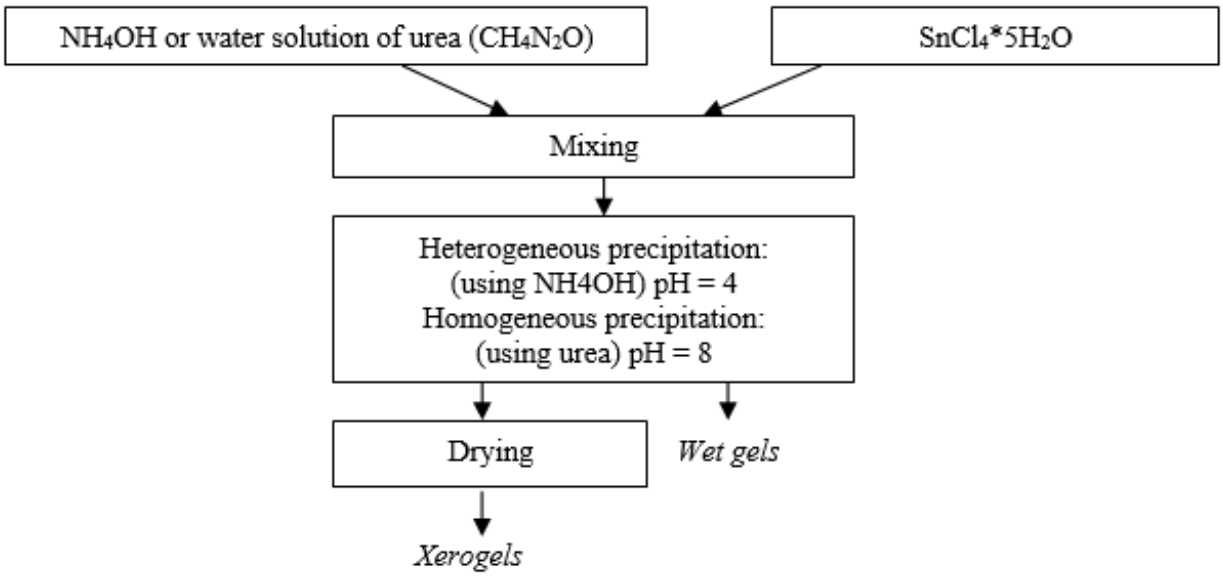

Fig. 1. The scheme for obtaining wet gels and xerogels of SnO_2 by hetero- and homogeneous precipitation

FTIR spectra were recorded using spectrophotometer "Spectrum-One" (Perkin-Elmer Instruments) in the range of 4000-400cm^{-1} in reflection mode. The adsorption-desorption isotherms of nitrogen were recorded using analyzer ASAP 2405N (Micromeritics Instrument Corp). The specific surface areas *S*, sorption pore volume V_s, micropores V_{mi} and mesopores volume V_{me} were calculated from isotherms using the BET, t- and the BJH methods. The total pore volume V_Σ was determined by ethanol impregnation of the samples granules dried at 150 °C. The volume of macropores V_{ma} was calculated as the difference between V_Σ and V_S. The diameter of the mesopores d_{me} was calculated from the pore size distribution curves (PSD) by the BJH method. UV-Vis spectra of the initial and modified samples SnO_2 in the wavelength range of 200-800 nm were obtained using a Lambda 35 UV - Vis spectrophotometer with Labsphere RSA-PE-20 attachment (Perkin-Elmer Instruments). The value of the band gap E_g was calculated according to Planck's formula (2):

$$E_g = \frac{1239.5}{\lambda}, \quad (2)$$

where λ is the absorption edge, nm.

Photocatalytic studies of modified samples. The study of the photocatalytic activity of all samples was carried out by the degradation of dyes (rhodamine B, safranin T) under the action of visible light in an aqueous medium ($1 \cdot 10^{-5}$ mol/l). Below are the structural formulas of the dyes used:

Rhodamine B

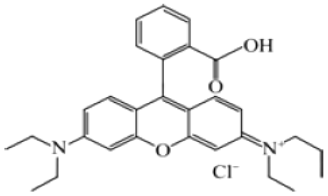

Safranin T

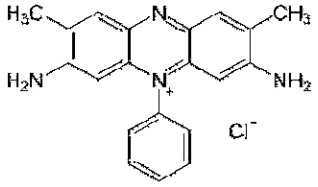

At first, to achieve adsorption equilibrium, the dye solution (80 ml) and the catalyst (80 mg) were stirred for 30 minutes in a glass reactor without irradiation. In the future, irradiation was carried out with a Philips LED Cool daylight LED lamp with a power of 100W for 10 hours. Sampling of irradiated solutions was carried out at certain time intervals. Catalysts were separated from the solution by centrifugation. A spectrophotometer UV-2450 (Shimadzu) was used to determine the dye concentration in these solutions. Photodegradation rate constants K_d were obtained by analyzing the change in optical density of the substrates solution at 553 and 520 nm for RhB and ST, respectively using the first-order kinetic equation. The degree of discoloration of solutions as criterium of substrates degradation was determined using spectrophotometric data. The degree of pollutants mineralization was calculated as decrease in the total organic carbon TOC [13, 14] using a TOC analyzer 5050A (Shimadzu).

Results and Discussion

Physicochemical properties. It was found that the initial precipitated and modified samples correspond to the composition of tin oxyhydroxide - $Sn_3O_4(OH)_4$. On the DTA-TG curves for the initial sample of the precipitated xerogel of tin oxyhydroxide (Fig. 2 a), it is possible to observe a mass loss of Δm_{exp} of 5.7 wt. % when the temperature is increased to 800 °C, which corresponds to the value of x = 1.15. Similar DTA-TG results were obtained when SnO_2 powder forms were obtained from hydroxides [15]. During mechanochemical treatment (MChT), partial removal of OH groups occurs, which is evidenced by a decrease in the value of the calculated coefficient *x* (Table 1). Microwave treatment (MWT), like MChT, but to a greater extent, helps to reduce the number of OH groups. A ratio of the number of structural OH groups to Sn for the modified sample is 0.53 (Table 1). However, in the latter case, the composition of the sample is closer to SnO_2. The obtained results are confirmed by IR spectroscopy.

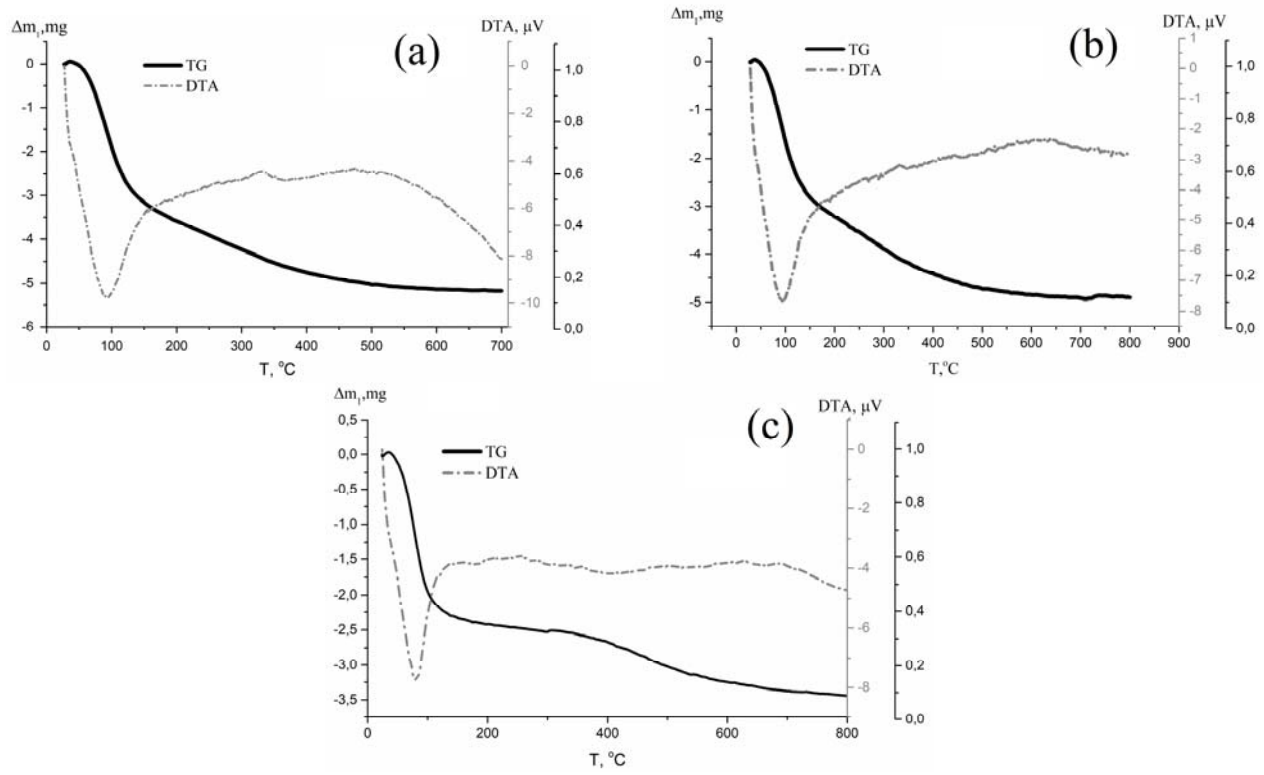

Fig. 2. The DTA–TG curves for tin oxyhydroxide: initial xerogel (a),that after MChT in air (b) and that after MWT gel

Table 1. Mass losses Δm_{exp} and coefficient x for initial and modified samples of $SnO(OH)_x$

Samples		x	Δm_{exp}, %
$SnO(OH)_x$	xerogel initial	1.15	5.7
	xerogel MChT air 600 rpm	1.13	5.6
	xerogel MChT H_2O 600 rpm	1.12	5.6
	gel MChT 600 rpm.	0.91	4.5
	gel MWT 235 °C 1 h	0.53	2.6

In FTIR spectra (Fig. 3) of the initial and modified samples $SnO(OH)_2$, absorption bands are observed in the area of vibrations of the frame and vibrations of OH groups. Thus, several absorption bands can be distinguished in the region of vibrations of the tin dioxide framework (700-400 cm^{-1}): at 660 and 579 cm^{-1}, which relate to the vibrations of bridging bonds in O-Sn-O and the Sn-O(H) terminal group, respectively [16-19]. Their position after MChT of heterogeneously and homogeneously precipitated samples changes by approximately 5-10 cm^{-1}, which indicates a certain disorganization of the structure of tin dioxide. As a result of the modification, the intensity of the absorption bands at 930 and 1245 cm^{-1}, which are related to the deformation vibrations of different types of OH-groups [20, 21], decreases. Similarly, the intensity of absorption bands decreases in the region of valence vibrations of OH groups (3000-3500 cm^{-1}). Thus, the greatest loss of OH groups occurs during MChT of gels. It should be noted that treatment speed contributes to this process. Similar results were obtained for SnO_2 powders after MChT [22]. Absorption bands at 1635 and 2430 cm^{-1} correspond to oscillation of C=O and residual CO_2 from the atmosphere, respectively [23].

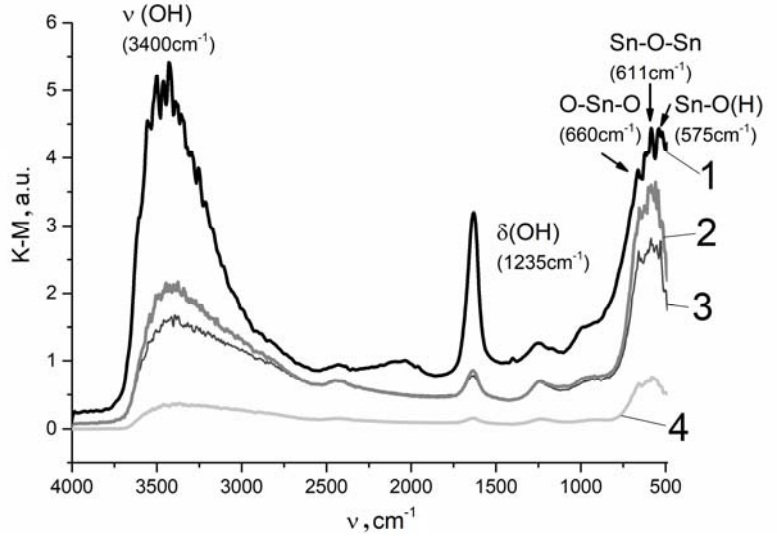

Fig. 3. FTIR-spectra of samples of the tin oxyhydroxide samples: initial (1) as well as those after MChT of xerogel in water (2), in air (3) and MChT of gel (4)

XRD analysis indicates that the initial sample has an imperfect crystal structure corresponding to the tetragonal modification of cassiterite (JCPDS (No. 41-1445)) (Fig. 4). During mechanochemical treatment, the phase composition of the samples does not change. Diffraction peaks (110), (101), and (211) at 2θ = 26.5°, 33.8°, and 51.9°, respectively, are observed both with dry MChT and with MChT in water. But at the same time, all modified samples are characterized by a slight increase in the intensity of reflexes, compared to the initial $SnO(OH)_2$ (Fig. 4, Table 2). This is probably related to the dispersion processes and changes in the structure of primary particles that occur during MChT. For example, the intensity of the reflex for the (110) plane (2θ = 26.5°) for sample after dry MChT increases by 1.8 times

compared to the initial $SnO(OH)_2$, and after MChT in water – by 1.4 times. In turn, the size of the crystallites increases when calculated in the direction of the (110) plane (Table 2).

Table 2. Crystallite sizes *L* and interplanar distances *d* for modified $SnO(OH)_2$ samples calculated by the Debye-Scherrer and Wolff-Bragg equations from XRD data

Samples		hkl	*L**, nm	β**, degree	d***, nm
$SnO(OH)_2$	initial	(110)	2.02	4.04	0.334
		(101)	3.14	2.64	0.265
		(211)	2.09	4.22	0.176
	MChT air 600 rpm	(110)	2.29	3.56	0.336
		(101)	3.22	2.58	0.265
		(211)	2.08	4.24	0.176
	MChT H_2O 600 rpm	(110)	2.05	3.97	0.329
		(101)	3.53	2.35	0.265
		(211)	2.03	4.35	0.176
	MWT xerogel 165 °C 0.5h	(110)	3.07	2.7	0.336
		(101)	2.55	3.2	0.264
		(211)	3.76	2.3	0.177
	MWT gel 185 °C 0.5h	(110)	2.20	3.7	0.333
		(101)	2.06	4.0	0.264
		(211)	2.51	3.5	0.176
	MWT gel 235 °C 1h	(110)	1.95	4.2	0.336
		(101)	1.85	4.5	0.265
		(211)	2.24	3.9	0.176
	MWT 270 °C	(110)	2.25	3.6	0.336
		(101)	1.98	4.2	0.265
		(211)	2.53	3.5	0.177

* L - crystallite size, nm; **β - width at half height of the peak, degree; ***d - interplanar distance, nm

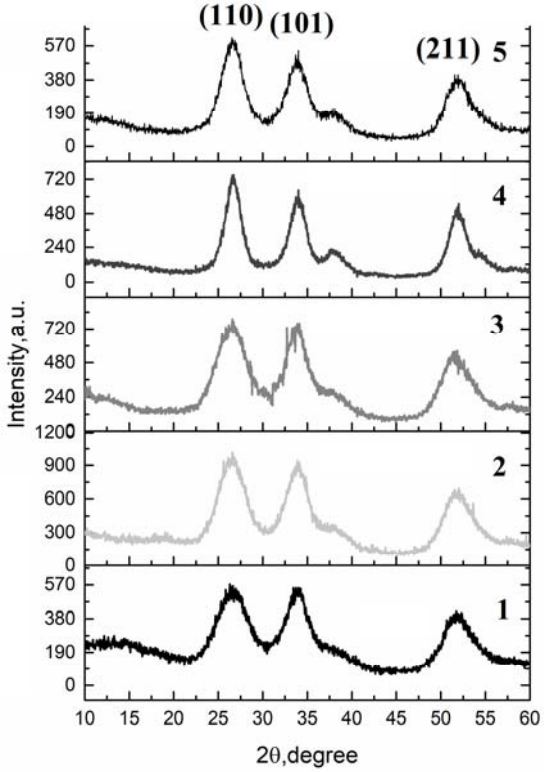

Fig. 4. XRD for samples tin oxyhydroxide: initial (1) and that after MChT in air (2), MChT in water (3), MWT of gel at 185 °C (4) and MWT of xerogel at 165 °C (5)

For samples of tin oxyhydroxide after MWT, with an increase in the treatment time and temperature, an increase in the intensity of reflexes *I* and the size of crystallites *L* is observed (Table 2), which correlates with the results of DTA-TG and indicates the processes of transformation of an amorphous crystalline structure into a more crystalline one, close to crystalline SnO_2. [24]. For example, the intensity of *I* reflexes for a sample after MWT in the gel stage at 185 °C for 0.5 h increases by 1.5 times, and at 235 °C and 95 atm for 1 h – by almost 3 times, compared to the initial sample. At the same time, the size of *L* crystallites increases by 2 times (Table 2). Similar processes occur during hydrothermal treatment, but at higher temperatures and during longer treatment [25].

Nitrogen adsorption-desorption isotherms and pore size distribution curves for the initial and modified samples $SnO(OH)_2$ are shown in Fig. 5 a, b. The isotherms of the initial tin oxyhydroxide samples belong to type I. For samples after dry MChT and MChT in water, they are close to type I. In turn, the isotherms of samples after MChT gels are similar to the initial ones, but a sharp rise is observed in the region of high values of $P/P_0 > 0.9$. The parameters of the porous structure of initial and modified samples $SnO(OH)_2$, calculated from the nitrogen adsorption-desorption isotherms, are given in Table 3.

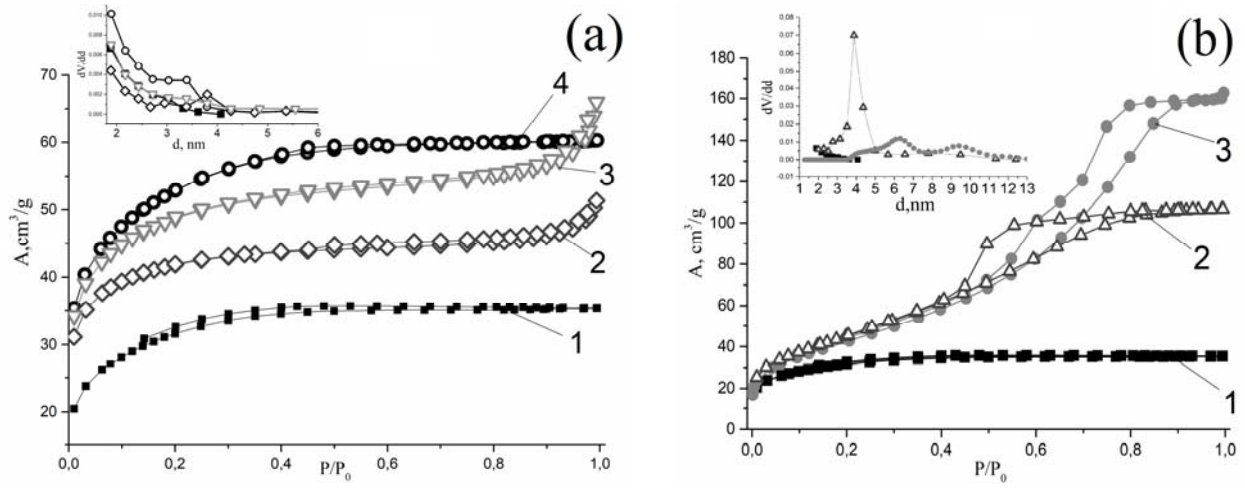

Fig. 5. N_2 adsorption-desorption isotherms and pore size distribution (BJH method) (inset) for $SnO(OH)_2$ samples (a): initial (1), after MChT air at 300 rpm (2), after MChT H2O at 300 rpm (3), after MChT gel at 300 rpm (4); (b): initial (1), after MWT xerogel at 165 °C (2), after MWT gel at 235 °C (3)

The initial samples have high specific surface area and a high content of micropores [25-27]. Dry MChT leads to a decrease in the specific surface area *S* and volume of micropores V_{mi}. At the same time, with MChT in water, there is an increase in V_Σ and a slight decrease in *S*. A feature of MChT of dry xerogel in water is the formation of secondary porosity represented by macropores, which is indicated by the excess of V_Σ values over the values of the sorption volume of V_S pores (Table 3). This effect of MChT on the porous structure corresponds to previously obtained results for other oxides and hydroxides [20, 28]. It should be noted that the parameters of the porous structure of the samples after MChT gels remain almost unchanged compared to the initial samples. A slight increase in the specific surface area and sorption volume is observed, as well as a slight decrease in the volume of mesopores and the size of primary particles.

The isotherms of the samples $SnO(OH)_2$ after MWT (Fig. 5 b) belong to different types. Thus, the isotherm of the sample after MWT at the wet gel stage at 185 °C for 0.5 h is close to type I. At the same time, the isotherms of other modified samples belong to type IV and have clearly defined

hysteresis loops close to types H2 and H3. This indicates that the mesoporous structure of tin dioxide is formed during MWT. Moreover, when $SnO(OH)_2$ is modified in the form of xerogels, a change in the type of isotherms is observed already after 0.5 h of treatment and at lower temperatures, compared to samples of tin oxyhydroxide modified at the gel stage. Similar trends are characteristic of SnO_2 after hydrothermal treatment [25, 29, 30]. The parameters of the porous structure calculated from the isotherms are given in Table 3. In the case of MWT of tin oxyhydroxide xerogel, the specific surface area S and volume of micropores V_{mi} decrease, the total V_Σ and sorption volume V_S of pores, the volume $V_{\text{ме}}$ and diameter $d_{\text{ме}}$ of mesopores increase. In turn, during the MWT gel of tin oxyhydroxide, a certain increase in the specific surface area S, an increase in the V_Σ and sorption volume V_S volume of pores, and the formation of meso- and macropores are observed within 0.5 h. During further processing for 1 hour, the specific surface area S decreases and the volume $V_{\text{ме}}$ and diameter $d_{\text{ме}}$ of mesopores increase.

Table 3. Influence of mechanochemical and microwave treatment on the parameters of the porous structure of initial and modified $SnO(OH)_2$ samples

Samples		S, m^2/g	V_Σ, cm^3/g	V_S, cm^3/g	V_{mii}, cm^3/g	V_{me}, cm^3/g	V_{ma}, cm^3/g	d_{me}, nm
$SnO(OH)_2$	initial	178	0.10	0.05	0.08	0.02	-	2.3
	MChT air 300 rpm	138	0.08	0.08	0.04	0.03	-	4.1
	MChT air 600 rpm	135	0.16	0.07	0.04	0.02	0.09	5.4
	MChT H_2O 300 rpm	163	0.33	0.10	0.04	0.05	0.23	4.3
	MChT H_2O 600 rpm	159	0.27	0.08	0.04	0.03	0.19	3.8
	MChT gel 300 rpm	180	0.17	0.09	0.04	0.04	0.08	2.4
	MChT gel 600 rpm	183	0.13	0.08	0.04	0.03	0.04	3.7
	MWT xerogel 165 °C 0.5 h	166	0.17	0.17	0.00	0.17	-	3.7
	MWT xerogel 175 °C 1 h	92	0.14	0.12	0.00	0.12	0.02	5.8
	MWT gel 185 °C 0.5 h	183	0.31	0.11	0.00	0.11	0.20	2.7
	MWT gel 235 °C 1 h	156	0.25	0.25	0.00	0.25	-	4.3

In the electronic spectra in the Kubelka-Munk coordinates (Fig. 6) for the initial and modified samples $SnO(OH)_2$, there are absorption bands that are characteristic of tin dioxide (260-290 nm) [20, 31-32] After MChT $SnO(OH)_2$, a bathochromic shift of the absorption edge is observed from 302 nm to 312 nm for the initial sample and after MChT in water, respectively (Table 4). This contributes to a decrease in the value of the band gap from 4.1 to 3.9 eV and an increase in light absorption from 14 to 19 % (Table 4).

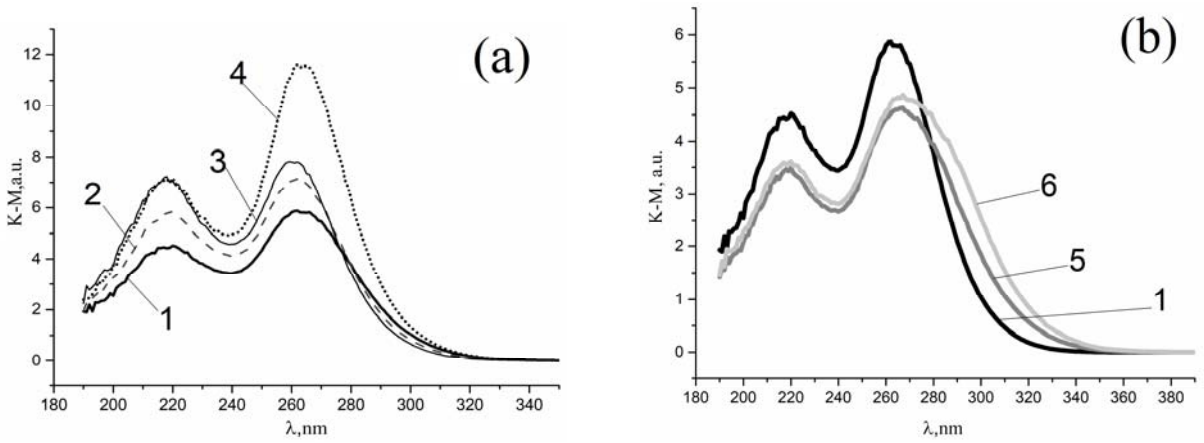

Fig. 6. UV- Vis spectra for SnO_2 samples: initial (1); after MChT in air (2), after MChT in H_2O (3), after MChT of gel (4), after MWT of xerogel (4) and gel (6)

After MWT, as after MChT, there is a shift of the absorption edge λ to the long-wave region from 302 nm to 335 nm for initial sample and the sample after MWT at the xerogel stage at 165 °C for 0.5 h, respectively. Due to this, there is a narrowing of the band gap to 3.56 eV (Table 4), and the absorption of visible light *A* increases by two times, compared to the initial sample. Such changes in electronic characteristics can be associated with the transformation of oxyhydroxide into tin dioxide, as well as the formation of structural defects [32].

Table 4. The effect of mechanochemical and microwave treatment on the electronic properties of initial and modified tin oxyhydroxide samples

Samples		λ *, nm	E_g **, eV	A***,%
$SnO(OH)_2$	initial	302	4.2	14
	MChT air 300 rpm	311	3.98	18
	MChT H_2O 300 rpm	312	3.97	19
	MChT gel 300 rpm	309	4.01	10
	MWT xerogel 165 °C 0.5 h	373	3.32	11
	MWT gel 185 °C 0.5 h	370	3.35	7

* λ - absorption edge, nm; ** E_g - band gap width, eV; ***A - light absorption at 550 nm, %

Photocatalytic activity. The previously described changes in the physicochemical characteristics of modified tin oxyhydroxide samples contributed to changes in their photocatalytic activity. Studies of the photocatalytic activity of the initial and modified samples show that the initial precipitated samples $SnO(OH)_2$ are inactive in the photodegradation processes of safranin T and methyl orange under the influence of visible light. Also, they have low photocatalytic activity in relation to rhodamine B, only partial deethylation of rhodamine B occurs. The degradation constants of rhodamine B are about $2*10^{-5}s^{-1}$, and the degree of decolorization in 2 h is 16-22 % (Table 5).

Table 5. Photocatalytic activity of modified tin oxyhydroxide samples

Samples	Rhodamine B		Safranin T	
	$K_d \times 10^5$, s^{-1}	Degree of discoloration, %	$K_d \times 10^5$, s^{-1}	Degree of discoloration, %
Initial	2.9	16	n.a.	n.a.
MChT air 300 rpm	93.2	96	1.5	78
MChT H_2O 300 rpm	101.0	95	3.3	86
MChT gel 300 rpm	49.6	98	1.6	60
MWT xerogel 165 °C 0.5 h	-	-	3.1	76
MWT xerogel 175 °C 1 h	-	-	3.2	71
MWT gel 185 °C 0.5 h	-	-	3.3	85
MWT gel 235 °C 1 h	-	-	3.3	83

* n.a. – non active

Modification of precipitated tin oxyhydroxide by MChT and MWT leads to an increase in photocatalytic activity under Vis-irradiation. This is confirmed by changes in the electronic absorption spectra of the solutions of the dyes used. It can be seen that stepwise deethylation of rhodamine B and degradation of rhodamine 110 at different rates are observed for samples of precipitated $SnO(OH)_2$ after MChT and MWT (Fig. 7). $SnO(OH)_2$ modified by MChT and MWT also acquires photocatalytic activity in the process of safranin T degradation under visible light (Fig. 8). Indicators of photocatalytic activity, namely: constants of photocatalytic degradation of rhodamine B and safranin T under visible

light and the degree of discoloration are given in Table 5.1. For example, the degradation rate constant K_d of rhodamine B increases from 0.2 to 10.1×10^{-4} s^{-1} (Table 5), and the degradation rate constant of safranin T reaches $(1.5\text{-}3.4)\times10^{-5}$ s^{-1} (Fig. 5). In turn, the degree of decolorization of dye solutions when using modified samples reaches 86-98 %.

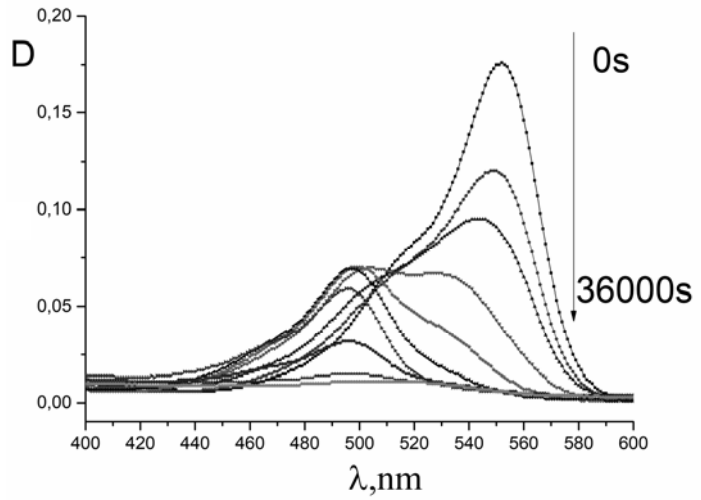

Fig. 7. Temporal spectral changes of RhB in the presence of $SnO(OH)_2$ sample after MChT of gel at 300 rpm

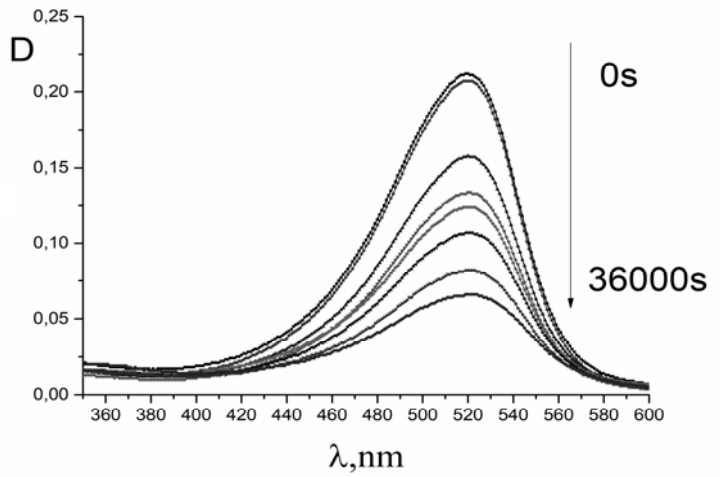

Fig. 8. Temporal spectral changes of safranin T in the presence of $SnO(OH)_2$ sample after MWT of the xerogel at 165 °C for 0.5 h

It was also shown that in the process of photodegradation of dyes, not only discoloration of solutions occurs, but also mineralization. The degree of mineralization is calculated by the decrease in the content of total organic carbon (TOC) and shows the degree of transformation of organic substances into less harmful inorganic ones. For modified samples of tin dioxide, the degree of mineralization of the studied dyes is 60-80 %. Probably, the increase in photocatalytic activity as a result of mechanochemical and microwave modification of the precipitated tin oxyhydroxide can be associated with the preservation of a high specific surface area, the formation and expansion of mesopores (from 2.3 to 5.4 nm), as well as the introduction of defects into the structure of the modified samples $SnO(OH)_2$ (Urbach tail). The latter causes an additional increase in dye adsorption on the surface of the photocatalyst and absorption of visible light by the photocatalyst. It is worth noting that the amount of adsorption of dyes increases monotonically with increasing intensity of tin oxyhydroxide treatments, and the band gap width Eg

decreases into varying degrees. An increase in the photocatalytic activity of the modified samples may indicate that visible light is absorbed by the dye, as a result of which the dye molecules are excited, followed by electron injection into the conduction zone of the photocatalyst, which is characteristic of the photosensitization process [33].

Conclusions

The work studied the modification of precipitated tin oxyhydroxide using mechanochemical and microwave treatments under various conditions and established the possibility of regulating its physicochemical characteristics. It was found that the application of mechanochemical and microwave treatment of tin oxyhydroxide at the wet gel stage leads to the formation of a homogeneous mesoporous structure with high values of specific surface area (178-183 m^2/g), pore volume (0.11-0.25 cm^3/g) and mesopore diameter (2.4-5.4 nm). In turn, mechanochemical treatment of xerogels in water allows to form a meso-macroporous structure. At the same time, microwave treatment contributes to the formation of a more perfect structure of the samples. Both types of modification help reduce the band gap of tin dioxide from 4.19 to 3.56 eV and increase the absorption of visible light by 2 times, due to the presence of structural defects (i.e., Urbach energy). As a result, the photocatalytic activity of modified samples of tin oxyhydroxide increases under the action of visible light.

Acknowledgements

The authors are grateful to the junior scientific researcher L. Kotynska (Institute for Sorption and Problems of Endoecology NAS of Ukraine, Kyiv, Ukraine) and doctor hab J. Skubiszewska-Zięba (Maria Curie-Skłodowska University, Lublin, Poland) for their help and support in the experiment.

References

1. Al-Hamdi A.M., Rinner U., Sillanpää M. Tin dioxide as a photocatalyst for water treatment: A review. *Process Saf. Environ. Prot. Institution of Chemical Engineers*, 2017, **107**, 190–205.
2. Miller T.A. et al. Nanostructured Tin Dioxide Materials for Gas Sensor Applications. *Funct. Mater.,* 2006, **5**, 1–24.
3. Orlandi M.O. Tin oxide materials. *Tin Oxide Materials* Elsevier Inc., 2020, **1**, 1–9.
4. Matushko I.P. et al. Sensitivity to hydrogen of sensor materials based on SnO_2 promoted with 3d metals. *Theor. Exp. Chem.,* 2008, **44**(2), 128–133.
5. Meng X. et al. Tin dioxide ion-gated transistors. *Tin Oxide Materials*. Elsevier Inc., 2020, **16**, 477–488.
6. Qin Y. et al. Post-synthetic modifications (PSM) on metal–organic frameworks (MOFs) for visible-light-initiated photocatalysis. *Dalton Trans.,* 2021, **50**, 13201–13215.
7. Leboda R., Charmas B., Sidorchuk V.V. Physicochemical and Technological Aspects of the Hydrothermal Modification of Complex Sorbents and Catalysts. Part I. Modification of Porous and Crystalline Structures R. *Adsorpt. Sci. Technol.,* 1997, **15**(3), 189–214.
8. Taylor P., Varma R.S. Green Chemistry Letters and Reviews “Greener” chemical syntheses using mechanochemical mixing or microwave and ultrasound irradiation. *Green Chem. Lett. Rev*., 2007, **1**(1), 37–45.
9. Yang G., Park S.J. Conventional and microwave hydrothermal synthesis and application of functional materials: A review. *Materials (Basel),* 2019, **12**, 1177.
10. Hinman J.J., Suslick K.S. Nanostructured Materials Synthesis Using Ultrasound. *Top. Curr. Chem*., 2017, **375**, 12.
11. Szczesniak B., Choma J., Jaronies M. Recent advances in mechanochemical synthesis of mesoporous metal oxides. *Mater. Adv.,* 2021, **2**, 2510–2523.

12. Hernández J.G. et al. European Research in Focus: Mechanochemistry for Sustainable Industry (COST Action MechSustInd). *Eur. J. Org. Chem.,* 2020, 8–9.
13. Vignesh K. et. al. Photocatalytic performance of Ag doped SnO_2 nanoparticles modified with curcumin. *Solid State Sci.,* 2013, **21**, 91–99.
14. Rauf M.A., Ashraf S.S. Fundamental Principles and Application of Heterogeneous Photocatalytic Degradation of Dyes in Solution. *Chemical Engineering Journal*, 2009, **151**, 10–18.
15. Ivanov V. et al. Synthesis of SnO_2 powders by decomposition of the thermally unstable compounds. Journal of Siberian Federal University. *Engineering & Technologies*, 2010, **3**(2), 189–213.
16. Sokovykh E.V. et al. Influence of temperature conditions of forming nanosized SnO_2-based materials on hydrogen sensor properties. *J. Therm. Anal. Calorim*, 2015, **121**(3), 1159–1165.
17. Zhang G., Liu M. Preparation of nanostructured tin oxide using a sol-gel process based on tin tetrachloride and ethylene glycol. *J. Mater. Sci*., 1999, **34**(13), 3213–3219.
18. Orel B. et al. Structural and FTIR spectroscopic studies of gel-xerogel-oxide transitions of SnO_2 and SnO_2:Sb powders and dip-coated films prepared via inorganic sol-gel route. *J. Non. Cryst. Solids*., 1994, **167**(3), 272–288.
19. Zhu J. et al. Sonochemical Synthesis of SnO_2 Nanoparticles and Their Preliminary Study as Li Insertion Electrodes. *Chem.Mater.,* 2000, **12**, 2557–2566.
20. Sergent N. et al. Preparation and characterisation of high surface area stannic oxides: structural, textural and semiconducting properties. *Sensors and Actuators B*: *Chemical*, 2002, **84**, 176.
21. Srivastava D.N. et al. Sonochemical Synthesis of Mesoporous Tin Oxide. *Langmuir*, 2002, **18**, 4160–4164.
22. Khalameida S. et al. Effect of mechanochemical modification on properties of powder tin(IV) oxide and oxohydroxide. *Chemistry, Physics and Technology of Surface*, 2017, **8**(3), 271–288. [in Ukranian].
23. Ho S.Y., Wong A.S.W., Ho G.W. Controllable porosity of monodispersed tin oxide nanospheres via an additive-free chemical route. *Cryst. Growth Des*., 2009, **9**(2), 732–736.
24. Akram M. et al. Continuous microwave flow synthesis and characterization of nanosized tin oxide. *Mater. Lett. Elsevier*, 2015, **160**, 146–149.
25. Gavrilov V. Adsorption research of microporous structure of tin dioxide. *Kinetics and Catalysis,* 2000, **41**(2), 304. [in Russian].
26. Gavrilov V., Zenkovets G. Influence of conditions of deposition of tin dioxide to form a porous structure of the xerogel. *Kinetics and Catalysis*, 1992, **33**(1), 183–189.
27. Acarbaş O., Suvaci E., Doğan A. Preparetion of nanosized tin oxide (SnO_2) powder by homogeneous precipitation. *Ceramics International*, 2007, **33**, 537–542.
28. Buyanov R., Molchanov V., Boldyrev V. Mechanochemical activation as a tool of increasing catalytic activity. *Catalysis Today*, 2009, **144**(3–4), 212–218.
29. Skwarek E. et al. Influence of mechanochemical activation on structure and some properties of mixed vanadium–molybdenum oxides. *J Therm Anal Calorim*, 2011, **106**, 881–894.
30. He Z., Zhou J. Synthesis, Characterization, and Activity of Tin Oxide Nanoparticles: Influence of Solvothermal Time on Photocatalytic Degradation of Rhodamine B. *Mod. Res. Catal*., 2013, **02**(03), 13–18.
31. Yuan H., Xu J. Preparation, Characterization and Photocatalytic Activity of Nanometer SnO_2. *Int. J. Chem. Eng. Appl.*, 2010, **1**(3), 241–246.
32. Kryukov A. et al. Nanophotocatalysis. Akademperiodyka, Kiev, 2013, 618. [in Russian].
33. Wu T. et al. Photoassisted degradation of dye pollutants. V. Self-photosensitized oxidative transformation of Rhodamine B under visible light irradiation in aqueous TiO_2 dispersions. *J. Phys. Chem. B,* 1998, **102**(30), 5845–5851.

Надійшла до редакції 31.07.2023

Вплив механохімічного та мікрохвильового модифікування на властивості SnO_2 як фотокаталізатора

Марія М. Самсоненко, Світлана В. Халамейда

Інститут сорбції та проблем ендоекології Національної академії наук України
вул. Генерала Наумова, 13, Київ, 03164, Україна, mashuna.08@gmail.com

Зразки осадженого SnO_2 модифікували за допомогою механохімічної та мікрохвильової обробки. Фізико-хімічні властивості всіх зразків були досліджені за допомогою ДТА, РФА, FTIR-спектроскопії, адсорбції-десорбції азоту та UV-Vis спектроскопії. Фотокаталітичну активність під дією видимого світла оцінювали за допомогою розкладу родаміну Б і сафраніну Т у водному середовищі. Показано, що вихідні осаджені та модифіковані зразки відповідають складу оксигідроксиду олова – $SnO(OH)_x$. Встановлено, що в результаті механохімічної та мікрохвильової обробки оксигідроксиду олова на стадії вологого гелю можна отримати фотокаталітично активні матеріали з однорідною мезопоруватою структурою та високими значеннями питомої поверхні та шириною забороненої зони близько 3.5-3.6 еВ. Особливістю механохімічної обробки ксерогелів у воді є утворення мезо-макропоруватої структури. Обговорено зв'язок між фізико-хімічними та фотокаталітичними властивостями модифікованих зразків. Встановлено залежність ефективності фотокаталітичної деградації барвників від зміни поруватої структури, наявності дефектів на поверхні фотокаталізатора та його електронних характеристик.

***Ключові слова**:* SnO_2, механохімічна та мікрохвильова обробка, порувата структура, фотокаталітична активність, барвники, видиме світло